AIP | Journal of Applied Physics

# Modeling of silicon nanocrystals based down-shifter for enhanced silicon solar cell performance

F. Sgrignuoli, G. Paternoster, A. Marconi, P. Ingenhoven, A. Anopchenko et al.

Citation: J. Appl. Phys. **111**, 034303 (2012); doi: 10.1063/1.3679140
View online: http://dx.doi.org/10.1063/1.3679140
View Table of Contents: http://jap.aip.org/resource/1/JAPIAU/v111/i3
Published by the American Institute of Physics.

# Modeling of silicon nanocrystals based down-shifter for enhanced silicon solar cell performance

F. Sgrignuoli,[1,a)] G. Paternoster,[2] A. Marconi,[1] P. Ingenhoven,[1] A. Anopchenko,[1] G. Pucker,[3] and L. Pavesi[1]
[1]*Nanoscience Laboratory, Department of Physics, University of Trento, Via Sommarive 14, 38123 Povo (Trento), Italy*
[2]*Department of Physics, University of Trento and Microtechnologies Laboratory, Bruno Kessler Foundation, Via Sommarive 18, 38123 Povo (Trento), Italy*
[3]*Advanced Photonics and Photovoltaics Group, Bruno Kessler Foundation, Via Sommarive 18, 38123 Povo (Trento), Italy*

(Received 7 September 2011; accepted 19 December 2011; published online 2 February 2012)

A transfer matrix model of a luminescent down-shifter (LDS) layer, consisting of silicon nanocrystals (Si-NCs) embedded in a silicon oxide matrix, on a silicon solar cells is presented. To enhance the efficiency of the silicon solar cell, we propose using a $SiO_2$/Si-NCs double layer stack, as an anti-reflection-coating (ARC) and as a LDS material. The optical characteristics of this stack have been simulated and optimized as a front surface coating. The cell performances have been simulated by means of a two-dimensional device simulator and compared with the performances of a reference silicon solar cell. We found a 6% relative enhancement of the energy conversion efficiency with respect to the reference cell. We demonstrate that this enhancement results from the lower reflectance and from the down-shifter effect of the Si-NCs activated coating stack. © *2012 American Institute of Physics*. [doi:10.1063/1.3679140]

## I. INTRODUCTION

A novel photovoltaic concept aims at achieving high efficiency solar cells by developing active layers which modify the energy of incoming photons to maximize the collection of the generated carriers.[1,2] One possibility is to implement nanometer sized structures in solar cells[3–6] where high energy photons are absorbed and low energy photons are emitted. This effect, named luminescence down shifter (LDS) effect, modifies the sunlight spectrum which reaches the solar cell. In conventional silicon solar cells, the internal quantum efficiency (IQE) shows a drop in the high energy range (280–450 nm). The LDS effect reduces this loss by shifting high energy photons to lower energy photons for which IQE has its maximum value. Hence, an increase of the energy conversion efficiency is obtained by exploiting the sunlight spectrum below 450 nm (see Fig. 1(a)). Modeling studies on the LDS effect based on CdSe nanocrystals and fluorescent dyes have shown that the energy conversion efficiency may increase by about 10%.[7,8] Experimental work has shown a 6% relative increase in conversion efficiency for coating a multi-crystalline silicon solar cell with fluorescent coloring agent.[9] These promising results motivate the present study.

Potential LDS materials must have the following properties:[3,4]

- a wide absorption band in the region in which the cell IQE is low;
- a narrow emission band coinciding with the maximum value of IQE; and
- a Stokes shift between absorption and emission in order to reduce re-absorption losses.

Silicon nanocrystals (Si-NCs) dispersed in a silicon oxide matrix are good candidates as a LDS material. They exhibit a wide absorption band below 450 nm, near infrared photoluminescence that originates from band-to-band recombination of quantum confined excitons,[10,11] transparency over a wide range of wavelengths (Fig. 1(b)), and good photo-stability. Moreover, their emission wavelength can be easily tailored by a size change.[10,12] A further advantage is that Si-NCs can be used both as a surface passivation layer[13] and as an ARC.[3] In the following, we refer to the Si-NCs rich $SiO_2$ layer with the acronym SRO (silicon rich oxide).

The aim of this work is to model LDS effect and to optimize a silicon solar cell coated on the surface by a $SiO_2$/SRO double layer stack. The model is based on the transfer matrix method in combination with a phenomenological approach describing the photoluminescence behavior of Si-NCs. We consider two different cells: a high performance laboratory and a standard performance commercial solar cell (Table I for details).

## II. SIMULATION METHOD

We used a two step approach based on two different but interconnected simulations:

(1) an optical simulation to compute the spectral modification of the sunlight caused by the surface coating and
(2) a two-dimensional electrical simulation to evaluate the solar cell performances.

The optical simulations are used to calculate the optimal thicknesses of the $SiO_2$/SRO double layer stack. The optimal values are obtained by minimizing the reflection while maximizing the LDS effect, i.e., maximizing the photon flux

a)Electronic mail: sgrignuoli@science.unitn.it.

 

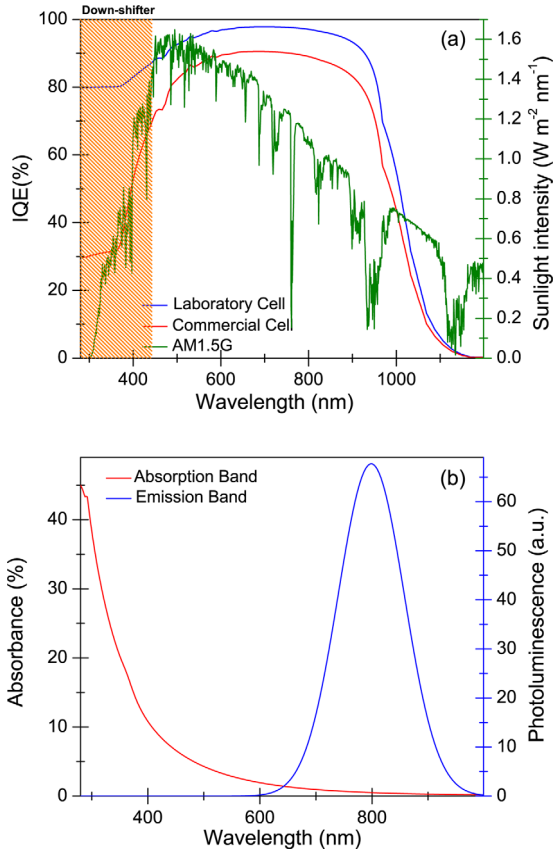


FIG. 1. (Color online) (a) AM1.5 G solar spectrum, simulated IQE of a laboratory, and a commercial solar cell. (b) Stokes shift between absorption and emission spectra of a Si-NCs layer. Data are taken from Ref. 18.

which arrives on the underlying silicon due to the Si-NCs absorption and emission. The photon flux is then used as a modified solar spectrum for evaluating the solar cell performances with the electrical simulation.

### A. Optical simulation

We used a transfer matrix approach to simulate the optical properties of the double stack layer.[14–16] The reflectance, transmittance, and absorbance of multilayered thin dielectric films are calculated by the optical admittance, $\mathcal{Y}$, which is defined by

$$\mathcal{Y} = \frac{C}{B}, \tag{1}$$

TABLE I. Main parameters of the laboratory (Lab. cell) and of the commercial (Com. cell) solar cell.

| Parameters | Lab. cell | Com. cell |
|---|---|---|
| Substrate | FZ p-type Si (1 Ohm cm) | CZ p-type Si (1 Ohm cm) |
| Cell thickness ($\mu$m) | 300 | 300 |
| Finger pitch ($\mu$m) | 400 | 2500 |
| Finger width ($\mu$m) | 10 | 150 |
| Front surface recombination velocity (cm/s) | $10^4$ | $4.5 \times 10^5$ |
| Sheet resistance (Ω/sq.) | 120 | 50 |

where $B$ and $C$ are the normalized electric and magnetic fields at the front surface and are calculated by using the formula

$$\begin{bmatrix} B \\ C \end{bmatrix} = \left\{ \prod_{r=1}^{q} \begin{bmatrix} \cos\delta_r & i\sin\delta_r/\eta_r \\ i\eta_r \sin\delta_r & \cos\delta_r \end{bmatrix} \right\} \begin{bmatrix} 1 \\ \eta_m \end{bmatrix}. \tag{2}$$

The suffix $m$ denotes the substrate or emergent medium while $\delta_r = 2\pi(n_r + ik_r)d_r \cos\theta_r/\lambda$ is the optical effective thickness of the rth layer. $n_r$ and $k_r$ are the real and the imaginary part of the refractive index, respectively, $d_r$ is the thickness, and $\theta_r$ is the angle with which the photons enter the rth layer. The various angles $\theta_r$ can be expressed as a function of the initial incidence angle using the generalized Snell's law.[17] $\eta_r$ is the optical admittance of the rth layer and it is the only parameter that depends on the polarization as

$$\eta_r^{TE} = \mathcal{Y}_0(n_r + ik_r)\cos\theta_r, \tag{3}$$

$$\eta_r^{TM} = \mathcal{Y}_0(n_r + ik_r)/\cos\theta_r, \tag{4}$$

where $\mathcal{Y}_0 = \sqrt{\varepsilon_0/\mu_0}$ is the optical admittance of free space.[14] $\varepsilon_0$ and $\mu_0$ indicate the vacuum permittivity and permeability, respectively. TE and TM stand for transverse electric and transverse magnetic polarized light. Equation (2) defines the characteristic matrix of a general structure and permits calculating its optical properties. The reflectance ($R$), transmittance ($T$), and absorbance ($A$) are given by

$$R = \left(\frac{\eta_0 B - C}{\eta_0 B + C}\right)\left(\frac{\eta_0 B - C}{\eta_0 B + C}\right)^*, \tag{5}$$

$$T = \frac{4\eta_0 \mathbb{R}e(\eta_m)}{(\eta_0 B + C)(\eta_0 B + C)^*}, \tag{6}$$

$$A = \frac{4\eta_0 \mathbb{R}e(BC^* - \eta_m)}{(\eta_0 B + C)(\eta_0 B + C)^*}, \tag{7}$$

where $\eta_0$ and $\eta_m$ are the optical admittance of the incident material and of the substrate, respectively.[14] These equations take into account the multiple-reflections and the multiple-transmissions that occur at the interfaces of a general multilayer stack.[14–16] We applied this formalism to a double-layer structure composed of a $SiO_2$ and of a SRO layer on a silicon substrate. Using the thicknesses and the refractive index $N(\lambda) = n(\lambda) + ik(\lambda)$ of air, $SiO_2$, SRO, and silicon as input, we calculated the reflection in air, the absorption in the active layer, and the transmission into the silicon substrate at normal and oblique incidence. The dielectric function and, hence, the refractive index, of the SRO layer were measured with variable-angle ellipsometry.[18] The refractive indices of the other materials were taken from the database of the thin film modeling software Scout®.[19]

The quantity which has to be maximized is the short circuit current ($I_{sc}$) of the coated silicon solar cell. $I_{sc}$ is calculated by the spectral responsivity ($\mathcal{SR}$) and by the spectral irradiance of AM1.5 G standard sunlight ($\mathfrak{S}$),[20,21] as follows:

$$I_{sc} = \int_{\lambda_{in}}^{\lambda_{fin}} d\lambda\, \mathcal{SR}(\lambda)\mathfrak{S}(\lambda)\mathcal{A}, \tag{8}$$

where $\mathcal{A}$ represents the area of the device while the $\mathcal{SR}$ is defined as

$$\mathcal{SR}(\lambda) = \frac{q\lambda}{hc} EQE(\lambda) = \frac{q\lambda}{hc} IQE(\lambda) T_{si}(\lambda), \quad (9)$$

where $q$ is the charge, $h$ the Plank constant, $c$ the velocity of light in vacuum, EQE is the external quantum efficiency, IQE denotes the internal quantum efficiency and $T_{si}(\lambda)$ expresses the transmission coefficient of the double layer stack. In presence of the LDS layer, the photon flux arriving at the silicon is modified by Si-NCs absorption and emission (Fig. 1(b)). Therefore, Eq. (9) has to be modified to take the Si-NCs emission into account as

$$\mathcal{SR}(\lambda) = \frac{q\lambda}{hc} [\mathcal{T}(\lambda) + \mathcal{T}_{PL}(\lambda)]. \quad (10)$$

The first term

$$\mathcal{T}(\lambda) = T_{si}^{n.i.}(\lambda) IQE(\lambda), \quad (11)$$

describes the part of the normal incidence radiation (*n.i.*) that is not absorbed by the active material. This fraction of light is transmitted directly into the silicon substrate and generates photocurrent. The second term

$$\mathcal{T}_{PL}(\lambda) = \mathcal{CE}\alpha(\lambda) \times \int_0^{\pi} \frac{d\phi}{\pi} \int_{\lambda_{in}}^{\lambda_{fin}} d\lambda' L(\lambda') T_{si}^{unp}(\lambda'; \phi) IQE(\lambda'), \quad (12)$$

expresses the Si-NCs emission. In more details,

- $\mathcal{CE}$ is the luminescence conversion efficiency. It represents the fraction of absorbed light that is emitted from Si-NCs. We can evaluate it by using the formula

$$\mathcal{CE} = \frac{\Gamma_{rad}}{\Gamma_{nr} + \Gamma_{rad}},$$

  where $\Gamma_{rad}$ and $\Gamma_{nr}$ are the radiative and non-radiative decay rates of the excitons in Si-NCs.[22] We assumed a conservative value of $\mathcal{CE} = 10\%$;[18]
- $\alpha(\lambda)$ is the optical absorption of the active material calculated by Eq. (7). It depends strongly on the geometry of the active material and on the size of Si-NCs (Fig. 1(b));
- $L(\lambda')$ is the experimental PL line-shape which is assumed to be a gaussian function

$$L(\lambda') = \frac{e^{(\lambda' - \lambda_{peak})^2 / 2\sigma^2}}{\sigma\sqrt{2\pi}}.$$

  where $\lambda_{peak} = 799$ nm is the PL peak wavelength while $\sigma = 58$ nm is the PL linewidth (Fig. 1(b)).
- $T_{si}^{unp}(\lambda; \phi)$ describes the contribution to the transmitted light due to the isotropic and unpolarized photons emitted by Si-NCs

$$T_{si}^{unp}(\lambda; \phi) = [\beta_{TE} T_{si}^{TE}(\lambda; \phi) + \beta_{TM} T_{si}^{TM}(\lambda; \phi)], \quad (13)$$

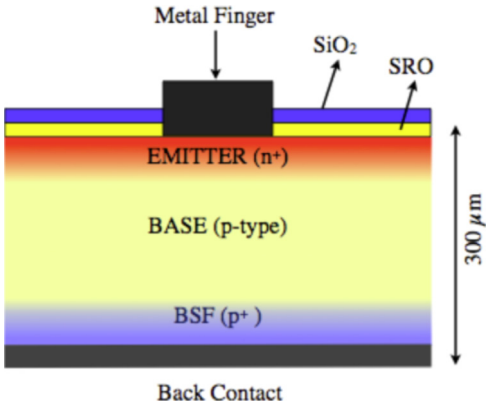


FIG. 2. (Color online) Cross section of a $n^+$-p-$p^+$ silicon solar cell with a $SiO_2$/SRO double layer stack coating (not in scale).

where $T_{si}^{TE}(\lambda; \phi)$ and $T_{si}^{TM}(\lambda; \phi)$ are the transmissions for a TE and TM polarization modes calculated using Eqs. (3), (4), and (6).[14–16] $\beta_{TE}$ and $\beta_{TM}$ express the fraction of *TE* or *TM* polarized photons. We assumed unpolarized light, i.e., $\beta_{TE} = \beta_{TM} = 0.5$.

### B. Electrical simulation

In order to evaluate the energy conversion efficiency enhancement due to the LDS effect, we performed two-dimensional numerical simulations of a cell under illumination by the modified solar spectrum. We used the SILVACO software tools.[23,24] Since the enhancement depends on the cell IQE, we considered two cells that have markedly different properties.

The first cell is a high efficiency laboratory cell realized on floating zone (FZ) p-type silicon substrate 300 $\mu$m thick and with 1Ω cm resistivity. The cell cross section is shown in Fig. 2. The phosphorous doping profile of the emitter and the boron back-surface-field (BSF) are optimized to minimize the surface recombination velocity.[25] 10 $\mu$m wide lines are opened in the passivating layer using photolithography and the metal fingers are deposited by sputtering. The second cell is a typical commercial silicon solar cell realized on Czochralski (CZ) p-type silicon. The metal grid is deposited by screen printing with a typical width of 150 $\mu$m. The phosphorous doping profile used here is standard for commercial solar cells.[26] The main characteristics of the cells are listed in Table I. Figure 1 shows the calculated IQE. The two cells have very different IQE, in particular for wavelength lower than 500 nm.

We calculated the I-V characteristics of these illuminated cells using the spectra modified by the active coating layer.

## III. RESULTS AND DISCUSSION

### A. Optimization of the double layer stack

The optimization of the $SiO_2$/SRO stack was carried out by finding the layer thicknesses that maximize the short circuit current of the solar cell. We used the simulated IQE of both the laboratory and commercial solar cell (see Fig. 1(a)) and Eqs. (8) and (10) to calculate $J_{sc}$ for different thickness values of $SiO_2$ and SRO. The thickness range investigated was 0 to 300 nm and 0 to 700 nm for $SiO_2$ and SRO,

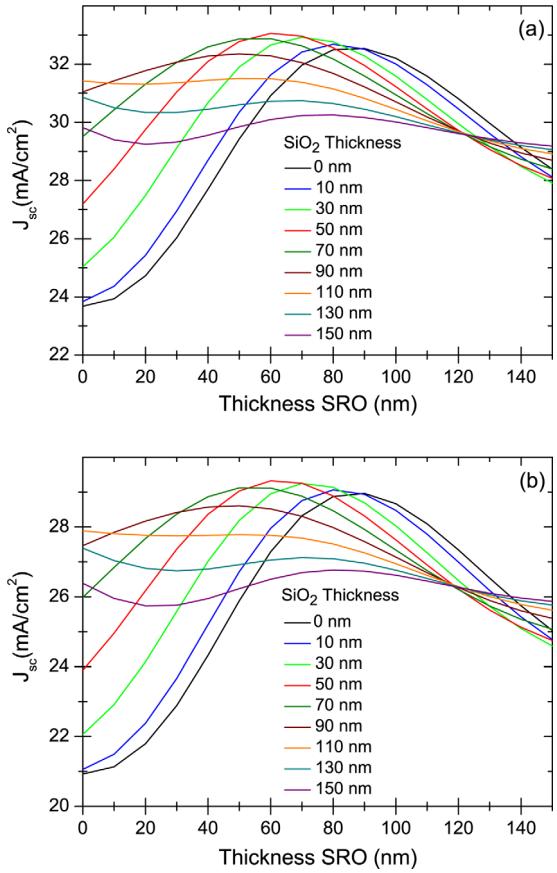


FIG. 3. (Color online) Short circuit current density as a function of the $SiO_2$ and SRO thickness of the laboratory (a) and commercial cell (b).

respectively. Figures 3(a) and 3(b) show the short circuit current density ($J_{sc}$) of both the laboratory and commercial solar cell as a function of the SRO thickness calculated using a $\mathcal{CE} = 10\%$ in Eq. (12). The color lines refer to different thickness values of the $SiO_2$ layer.

The dependence of $J_{sc}$ on the SRO and $SiO_2$ thicknesses is ruled by the double layer stack transmittance, the emission of the Si-NCs, and the IQE of the solar cell (Eqs. (8) and (10)). For thin SRO layer, maxima are observed in $J_{sc}$, see Fig. 3. For a given $SiO_2$ thickness value, a different SRO value maximizes $J_{sc}$ (Fig. 4(a)). In fact, interference effects, which depend both on the refractive index and thickness of each layer, account for the oscillatory behavior of $J_{sc}$. Different thickness combinations produce different phases between the wave reflected from the double layer stack top surface and the wave reflected from the SRO/Si interface. This thickness dependent effect explains the different thicknesses at which the short circuit current has a maximum in Fig. 3. Moreover, Fig. 3 shows that the presence of an active SRO layer increases $J_{sc}$ with respect to the bare $SiO_2$ single layer. These results prove that a cell coated with a $SiO_2$/SRO double layer stack shows a better performance than a cell coated with a single SRO layer. The maximum $J_{sc}$ obtained with a single SRO layer (black line) is lower than the one obtained with the double layer stack. Note also in Fig. 4(b) that the higher $\mathcal{CE}$ the thicker (thinner) is the SRO ($SiO_2$) thickness.

TABLE II. Optimized thickness values of the laboratory and commercial solar cell for a $\mathcal{CE} = 10\%$.

| | $SiO_2$ thickness (nm) | SRO thickness (nm) |
|---|---|---|
| Laboratory cell | $51 \pm 0.5$ | $62 \pm 0.5$ |
| Commercial cell | $48 \pm 0.5$ | $64 \pm 0.5$ |

The optimum stack parameters are summarized in Table II. The difference between these optimized combinations is due to the different IQE of the laboratory and the commercial solar cells (see Fig. 1(b)). In fact, the IQE enters into the thickness optimization of $J_{sc}$ via Eqs. (11) and (12). It is found that the two thickness combinations differ only by few nanometers. This means that the double layer stack works as a good ARC independently of the IQE of the specific solar cells. On the other hand, the LDS effect is critically dependent on the IQE which must be considered in the optimization simulations.

### B. Effect of LDS on the energy conversion efficiency

To further investigate the energy conversion efficiency enhancement, we studied three different implementations of the cells: (1) the laboratory and the commercial cell with the optimum layer stack (named ACTIVE cell); (2) the cells with the optimum layer stack where $\mathcal{CE} = 0$ (named PASSIVE cell); and (3) a reference cell coated with an ARC layer formed by a 107 nm thick $SiO_2$ layer (named REF cell). This $SiO_2$ thickness maximizes $J_{sc}$. The PASSIVE cell is used to single out the role of the Si-NCs emission from the combined ARC action of the double stack structure. Therefore, these three different implementations allow demonstrating the performance improvement of the ACTIVE cell with respect to the others. Note that the three cells have the same IQE.

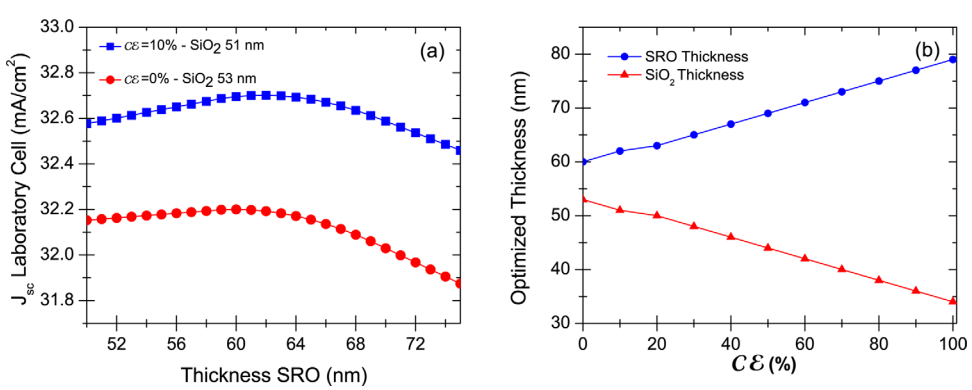


FIG. 4. (a) (Color online) $J_{sc}$ of the laboratory cell as a function of the SRO thickness for two $SiO_2$ thicknesses with and without the LDS effect. (b) Optimized thickness combinations that maximize the $J_{sc}$ of the laboratory solar cell as a function of the conversion efficiency of the Si-NCs.

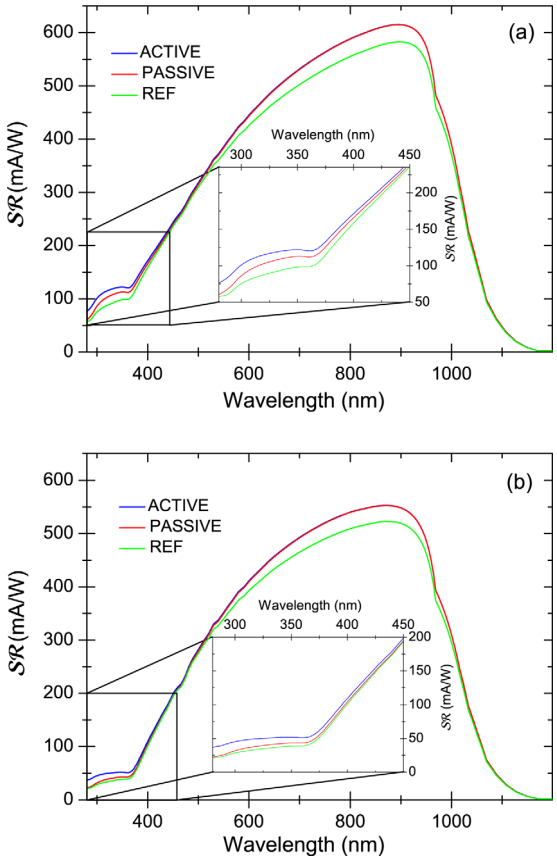


FIG. 5. (Color online) Spectral responsivity of the laboratory (a) and commercial (b) solar cells. The inset is a zoom in the short wavelength region.

Figures 5(a) and 5(b) show $\mathcal{SR}$ of the various cells. This parameter allows the detection of the LDS effect. An increase in the short wavelength range of the $\mathcal{SR}$ is expected for a cell formed by a Si-NCs active layer due to the LDS effect. The amount of this enhancement depends on the IQE of the solar cell. In more details, the LDS effect is more efficient in a cell with a low blue-IQE and a high red-IQE behavior. The ratio between them determines the increase of the solar cell efficiency due to the LDS effect. An effective increase of $\mathcal{SR}$ is observed for the short wavelengths due to the LDS effect. The laboratory and commercial cell show a relative enhancement of 6.5% and 10.6%, respectively. This enhancement was computed comparing the integral of the spectral responsivity for the ACTIVE and PASSIVE cells over the wavelength range 280–450 nm, i.e., where Si-NCs absorb. The enhancement due to the LDS effect is higher in the commercial cell with respect to the laboratory cell, because the commercial solar cell has a lower IQE in the UV-blue region than the laboratory IQE and a similar IQE in the red.[27] However, the best parameters of the laboratory cell produce a higher laboratory $\mathcal{SR}$ with respect to the commercial cell (see Table I).

Using the AM1.5 G solar spectrum[28] to illuminate the solar cell, the electrical parameters of the cell can be simulated. Figure 6 shows the modified solar spectra that reach the silicon for the REF (green curve), PASSIVE (red curve), and ACTIVE (blue curve) cells. Interestingly, more light

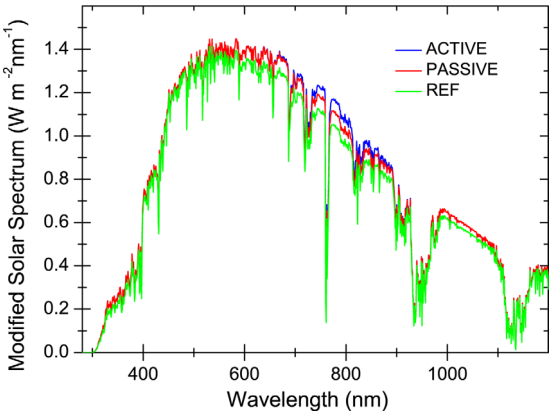


FIG. 6. (Color online) Modified solar spectra for the REF, PASSIVE, and ACTIVE laboratory cells, respectively.

reaches silicon when the double stack structure is used. In addition, considering the Si-NCs emission, a further increase is observed at about 750 nm. This is a direct evidence of the down-shifter effect in Si-NCs: photons absorbed in the blue are re-emitted in the red.

Figure 7 shows the IV characteristics of the laboratory (a) and commercial (b) solar cells under AM1.5 G illumination, respectively. The open circuit voltage and the fill factor do not change due to the different cells since the electrical properties of the cells are unaffected by the coating layer.[4] Yet, we obtained an overall enhancement in the energy conversion efficiency from 16.50% to 17.56% between the REF and ACTIVE laboratory cells and from 14.20% to 15.11% between the REF and ACTIVE commercial cells due to the increased short-circuit current density. These values correspond to a relative improvement of 6.44% and 6.36% for the laboratory and commercial cells. Comparing the ACTIVE and PASSIVE cells, it is possible to single out the contribution of the down-shifter effect to these values. We find 1.47% for the laboratory and 1.52% for the commercial cell.

To further investigate the Si-NCs contribution in the energy conversion efficiency, we changed the fraction of shifted photons, i.e., $\mathcal{CE}$. A Si-NCs conversion efficiency up to 60% has been reported in Ref. 22 As shown in Fig. 8, the relative enhancement due to the down-shifter effect increases linearly with respect to $\mathcal{CE}$. The energy conversion efficiency of the laboratory cell increase from about 17% to approximately 20%.

Previous modeling studies have shown an increase of approximately 10% in the energy conversion efficiency due to the LDS effect.[7,8] On top of the fact that these studies have been done for CdSe nanocrystals and fluorescent dye coating, there are other important differences to the present study. In Ref. 7, the energy conversion efficiency is evaluated using the integral of the modified solar spectra as the input power. This method produces a smaller spectral density than 0.1 W/cm$^2$, the value we used, and therefore, overestimates the energy conversion efficiency. Moreover, 3/4 of the emitted photons is assumed directed toward the underlying solar cell due to the internal reflection in the down-shifter layer independently from the wavelengths, whereas in

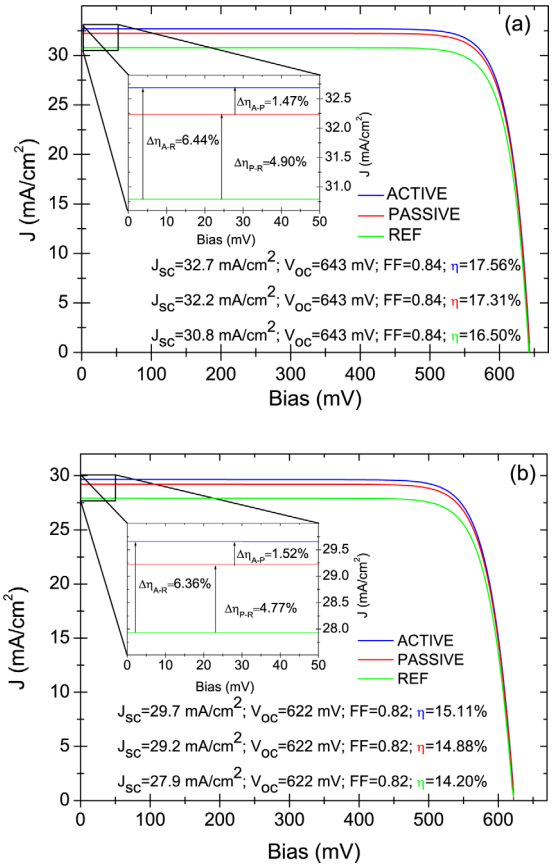


FIG. 7. (Color online) IV characteristics of the laboratory (a) and commercial (b) cells. The insets show the enhancement of $J_{sc}$ due to the LDS effect. $\Delta\eta_{A\text{-}P}$, $\Delta\eta_{P\text{-}R}$, and $\Delta\eta_{A\text{-}R}$ refer to the relative variations in the energy conversion efficiency between the ACTIVE-PASSIVE, PASSIVE-REF, and ACTIVE-REF cells, respectively. The differences between the laboratory and commercial solar cells are due to the difference in the optimized thickness combinations as well as to the different simulation parameters (see Table. I).

our model, we compute this ratio for each frequency and for each emission angle. The model presented in Ref. 8 is characterized by a conversion-collection factor evaluated as the product of the conversion efficiency with a collection probability factor. This quantity is assumed equal to the integral of the emissivity. In our model, we avoid these assumptions: the amount of emitted photons arriving in the substrate is calculated by the optical software itself (see Eq. (12)). Furthermore, in Refs. 7 and 8, the authors assume a conversion efficiency of their CdSe nanocrystals and fluorescent dyes of about 80%. Our results shown a relative enhancement of $\simeq 12\%$ for a $\mathcal{CE} = 80\%$ (see Fig. 8).

## IV. CONCLUSION

In this work, we simulated the properties of a $SiO_2$/SRO double layer stack as a front surface coating to improve the performances of silicon solar cells. The short circuit current was used as an optimization gauge to select the best thicknesses of the layers. It was found that a two layer stack gives better ARC than a single layer stack. In addition, even when high IQE is assumed, a significant down shifter effect is observed for Si-NCs: 1.47% of relative enhancement in the energy conversion efficiency for a 10% of shifted high energy photons. Furthermore, we demonstrated a linear relation between the down shifter effect and the luminescence conversion efficiency of the Si-NCs.

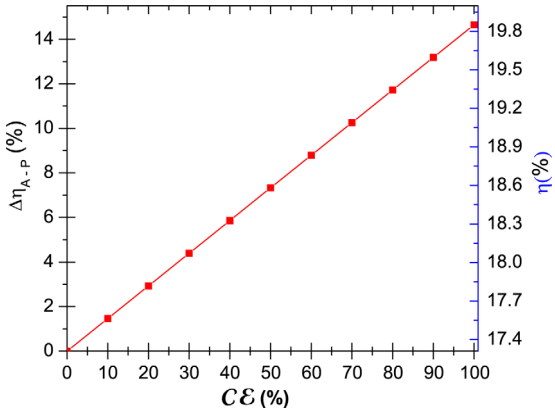


FIG. 8. (Color online) Relative enhancement in the energy conversion efficiency for the laboratory cell due to the down-shifter effect ($\Delta\eta_{A\text{-}P}$) as a function of the $\mathcal{CE}$, i.e., the fraction of shifted photons. The right axes expresses the total energy conversion efficiency ($\eta$) for the laboratory cell.

## ACKNOWLEDGMENTS

This work is supported by EC through the FP7 ICT-248909 LIMA project.

[1]P. Frankl, *Technology Roadmap: Solar photovoltaic Energy* (IEA, Paris, France, 2010).
[2]M. A. Green, *Third Generation Photovoltaics: Advanced Solar Energy Conversion* (Springer, Berlin, Germany, 2003).
[3]C. Strumpel, M. McCann, G. Beaucarne, V. Arkhipov, A. Slaoui, V. Svrcek, C. del Canizo, and I. Tobias, Sol. Energy Mater. Sol. Cells **91**, 829 (2007).
[4]E. Klampaftis, D. Ross, K. R. McIntosh, and B. S. Richards, Sol. Energy Mater. Sol. Cells **93**, 1182 (2009).
[5]V. Švrček, A. Slaoui, and J. Muller, Thin Solid Films **451–452**, 384 (2004).
[6]M. A. Green, Mater. Sci. Eng. B **74**, 118 (2000).
[7]W. G. J. H. M. v. Sark, A. Meijerink, R. Schropp, J. van Roosmalen, and E. Lysen, Sol. Energy Mater. Sol. Cells **87**, 395 (2005).
[8]G. C. Glaeser and U. Rau, Thin Solid Films **515**, 5964 (2007).
[9]T. Maruyama and J. Bandai, J. Electrochem. Soc. **146**, 266 (1999).
[10]L. Pavesi and T. Rasit, *Silicon Nanocrystals: Fundamentals, Synthesis and Applications* (Wiley-VCH Verlag GmbH, Berlin, Germany, 2010).
[11]M. V. Wolkin, J. Jorne, and P. M. Fauchet, Phys. Rev. Lett. **82**, 197 (1999).
[12]S. Ossicini, L. Pavesi, and F. Priolo, *Light emitting Silicon for Microphotonics* (Springer, Berlin, Germany, 2003).
[13]A. Aberle, *Crystalline Silicon Solar Cells: Advanced Surface Passivation and Analysis* (Centre of Photovoltaic Engineering, UNSW, Sidney, 1999).
[14]H. A. Macleod, *Thin Film Optical Filters*, 3rd ed. (IoP, Bristol, 2001).
[15]M. Bass, *Handbook of Optics*, 3rd ed., Vol. *IV*: *Optical Properties of Materials, Nonlinear Optics, Quantum Optics* (McGraw-Hill, United States, 2010).
[16]M. Born and E. Wolf, *Principles of Optics*, 7th ed. (Cambridge University Press, Cambridge, United Kingdom, 1999).
[17]L. D. Landau and E. M. Lifshitz, "Course of theoretical physics," in *Electrodynamics of Continuous Media*, 2nd ed. (Elsevier Butterworth-Heinemann, Oxford, 2004), Vol. 8.
[18]Z. Yuan, G. Pucker, A. Marconi, F. Sgrignuoli, A. Anopchenko, Y. Jestin, L. Ferrario, P. Bellutti, and L. Pavesi, Sol. Energy Mater. Sol. Cells **95**, 1224 (2011).
[19]W. Theiss, SCOUT *Optical Spectrum Simulator*, see http://www.wtheiss.com/?c=1&content=scout.
[20]A. Luque and S. Hegedus, *Handbook of Photovoltaic Science and Engineering* (Wiley, New York, 2003).

[21]S. R. Wenham, M. A. Green, M. E. Watt, and R. Corkish, *Applied Photovoltaics*, 2nd ed. (Earthscan, London, 2007).
[22]R. J. Walters, J. Kalkman, J. Polman, A. Atwater, and M. J. A. de Dood, Phys. Rev. B **73**, 132302 (2006).
[23]ATLAS User's Manual, Vols. 1-2, software version 5.6.O.R, Silvaco International, Sunnyvale, CA, 2003.
[24]M. Zanuccoli, P. F. Bresciani, M. Frei, H.-W. Guo, H. Fang, M. Agrawal, C. Fiegna, and E. Sangiorgi, *paper presented at the Photovoltaic Specialists Conference (PVSC)* (2010), 35th IEEE, pp. 2262–2265.
[25]A. Cuevas and D. Russel, Prog. Photovoltaics 8 (2000).
[26]M. M. Hilali, A. Rohatgi, and S. Acher, IEEE Trans. Electron devices **51**, 948 (2004).
[27]J. Yoann, G. Pucker, M. Ghulinyan, L. Ferrario, P. Bellutti, A. Picciotto, A. Collini, A. Marconi, A. Anopchenko, Z. Yuan, and L. Pavesi, Proc. SPIE, **7772**, 77720B (2010).
[28]ASTM G173-03 Reference Spectra derived from SMARTS v. 2.9.2, see http://rredc.nrel.gov/solar/spectra/am1.5/ASTMG173/ASTMG173.html.